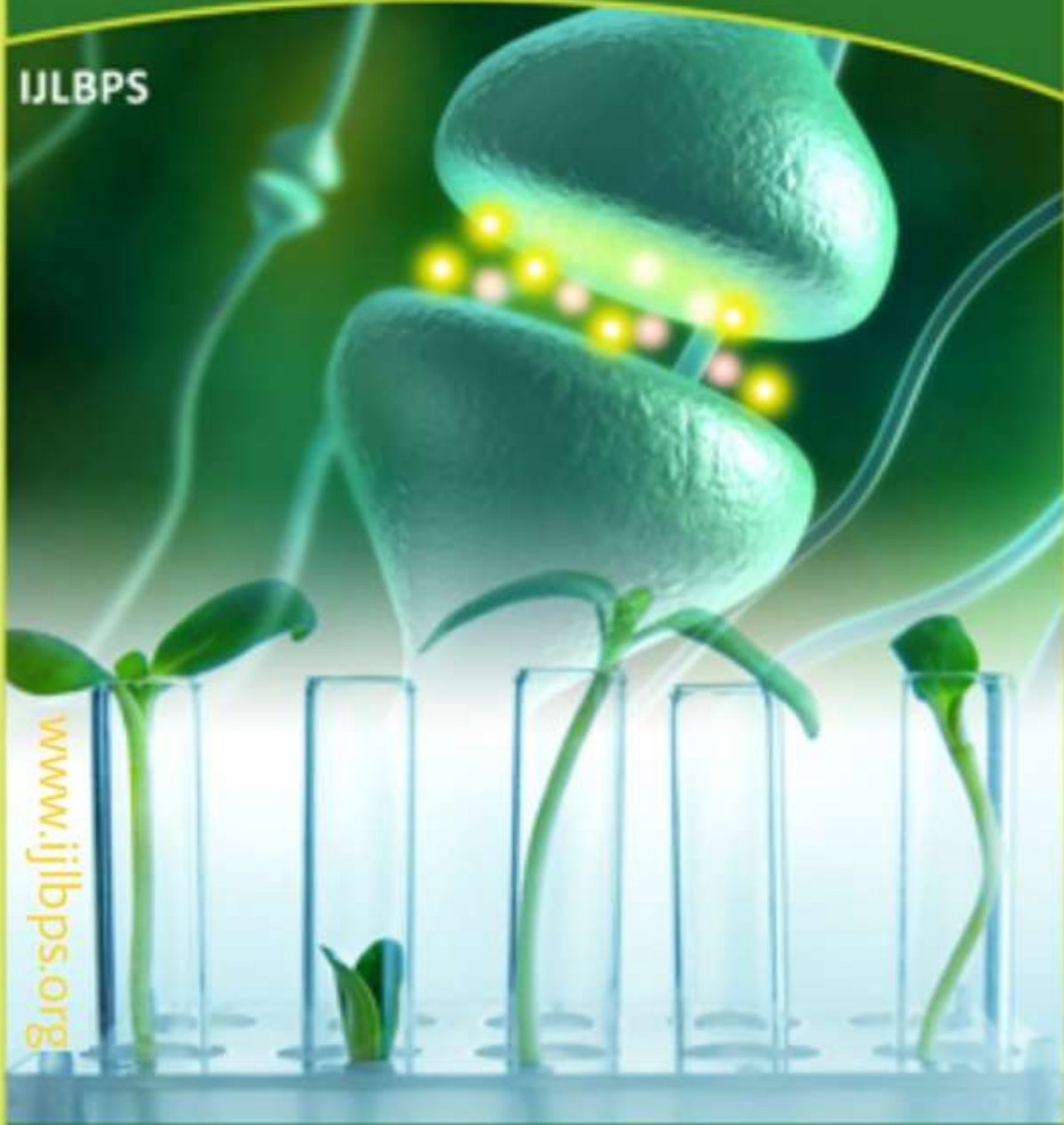




ISSN 2395-650X

**International Journal** of  
Life Sciences Biotechnology Pharma Sciences

IJLBPS



[www.ijlbps.org](http://www.ijlbps.org)

E-mail: [editorijlbps@gmail.com](mailto:editorijlbps@gmail.com) [editor@ijlbps.org](mailto:editor@ijlbps.org)

## Realization of SRM for High Speed EV Applications using Vector Control

1SyedaParveen Sulthana,2R. Yedukondalu

1PGScholar, 2Associateprofessor

1,2Department of Electrical and Electronics Engineering, Dr. Samuel George institute of engineering and technology, Prakasam,A. P, India

1spsulthana232@gmail.com,2santoshpaul717@gmail.com

---

### Abstract

Reduce the size of the motor by using a high-speed motor in an electric vehicle (EV). Switched There are various ways to describe reluctance, including the term "reluctance." Because of the rotor, the motor is able to drive at high speeds. Despite its simplicity, the design is effective. The drive theory, on the other hand, produces a great deal of acoustic noise during acceleration and background. Torque management, on the other hand, is a challenging task in the case of difficult current excitation. These concerns have been addressed by the use of vector control for SRM drive. Despite this, vector control has not been incorporated into the SRM for high-speed motors. This page explains the driving conditions for the SRM in the high-speed area, including the switching frequency and the bus voltage required. Vector control has been shown to be able to power the proposed SRM in the high-speed sector.

---

**Keywords:** High-speed drive with switched reluctance motor and vector control.

---

### Introduction

Many people are already driving electric vehicles (EVs) as a means of cutting back on their energy consumption. Downsizing a motor system for EV traction motors is required in order to increase electric power consumption and retain effective space in the motor room. One way to reduce the size of a motor is to increase its speed [1]. The output power of a motor is the product of torque and rotation. PMSMs utilising rare earth magnets are a symbol of EV traction

motors because of their great torque density and dependability. On the other hand, PMSMs are rife with danger. Rare earth metals in the rotor require a large production cost. Because the mechanical strength of the piercing is so weak, the high-speed drive is constrained. PMSMs could be replaced by SRMs (Switched Reluctance Motors) [2].

In both the stator and rotor, SRMs have powerful pole forms that are merely composed of an iron core and winding. Since SRMs have a simple and sturdy mechanism,

they can move at high speeds. Manuscript review began on the 15th of October 2019 with the submission of the document. Waseda University's School of Advanced Research and Engineering's department of electrical engineering and bioscience has an assistant professor named Kohei Aiso on its faculty. Professor Kan Akatsu teaches at Yokohama National University. They are able to reduce the size of the motor while still achieving high output power. For the traction motor, numerous SRMs have been registered. High-silicon steel was used to build the SRM, which has a 50 kW output capacity from 1200 to 6000 r/min and high torque density. [3] The SRM is the same size as the PMSM in the second-generation Toyota Prius [3]. High peak power is achieved by operating at 30000 rpm for the 80kW SRM with amorphous steel sheet rather than by using PMSMs. High performance can also be achieved by decreasing iron loss by using amorphous steel sheet [4].

For in-wheel EVs, a 12/26 pole SRM with high specific torque has also been proposed [5]. The volume of the end-winding and the depletion of copper, the SRM, will be affected by this.

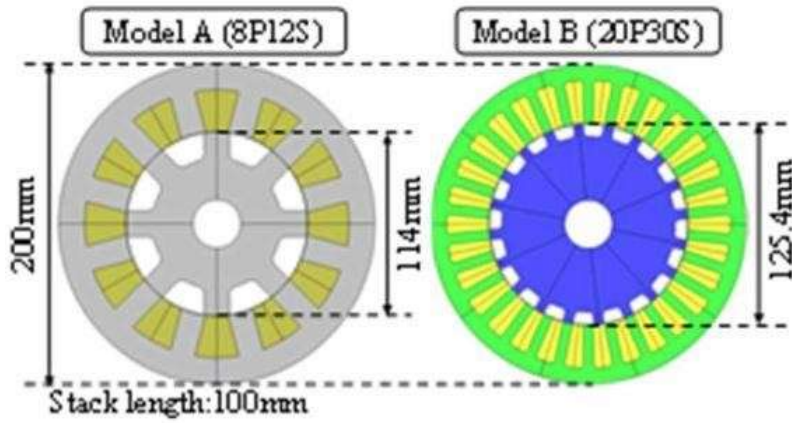
1. has accomplished motor reduction and excellent efficiency by utilizing a segmented outer rotor structure and a concentrated winding design. Due to the normal driving technique, SRMs are plagued with a plethora of hazards. Unipolar current is typically used to power SRMs. The current excitation begins at the point that the rotor poles begin to coincide with the stator poles when employing the hysteresis regulation or the voltage single pulse motor. The rotor and stator poles are then separated until they are perfectly aligned.

2. Excitation of the unipolar current is therefore discontinuous because of this fact. Because of the discontinuous current excitation, the SRMs produce a great deal of vibration and acoustic noise. By altering the radial force between the rotor pole and the stator pole, substantial vibrations can be generated when the voltage is abruptly cut off [6]. Reduction in vibration has been documented. Due to its sophisticated unipolar current excitation, the torque controller configuration is difficult. Certain regulated parameters, such as the turn-on angle, turn-off angle, and current chopping level, must be refined simultaneously [7]. Certain parameters must be set for each drive state in variable-speed applications in order to meet the requirements. These concerns have been addressed using a vector control for SRM [8]. To each circuit, SRM vector power applies sinusoidal current with a DC offset as the unipolar excitation current. The excitation current is comprised of both DC and AC components. In order to drive the SRM in the same way as conventional AC machines, these components generate the virtual rotor flux and spinning stator field [9]. Another benefit of vector control's continuous current excitation is a reduction in SRM vibration and noise [10]. Contrary to popular belief, vector control has not been used to SRMs powered by high-speed drives, as the parameters of the drive, such as bus voltage and switching frequency, are discussed in this study. It is also possible to use vector control in the high-speed zone of the proposed SRM to achieve high output power and reduced vibration. Ultimately, we want to put the 8pole 12-slot SRM that's been sitting on the bench to the test. Consequently, a 20-pole, 30-slot SRM with the same electrical frequency as an 8-pole, 12-slot SRM with a 50000rpm drive is presented in this work, and its vector control output is tested.

### 3. ProposedSRM

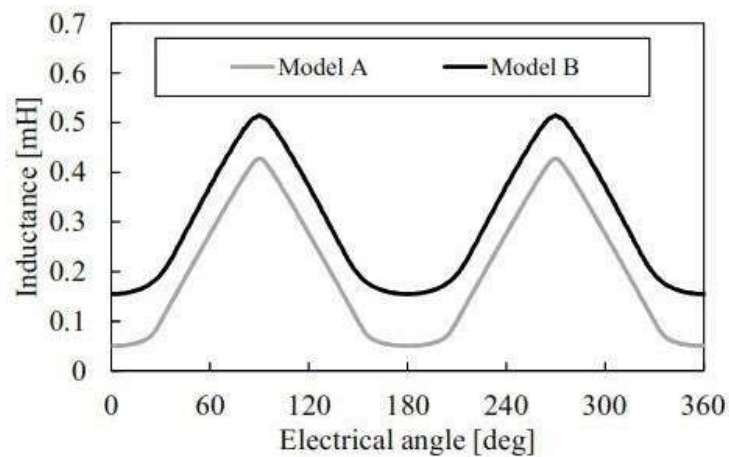
Figure 1 displays the 8 pole 12 slot SRM (model A), which has a maximum rotationspeedof50000rpm, and

the20pole 30slotSRM(modelB),whichhas a maximumrotation speedof20000rpm,withmeasurementsin TableI.



S.No	Parameters	Model A	Model B
1	Pole/Slot	8 /12	20/30
2	Outputpower[kW]	85	34
3	Maximumspeed[rpm]	50000	20000
4	Airgaplength[mm]	0.5	0.5
5	Numberofturns[turn/teeth]	5	5
6	Diameterofcoil[mm]	6.0	4.0
7	Resistance[Ω/phase]	0.003	0.018
8	Corematerial	-	20H1200

**Table1.SpecificationofProposedSRM**



The electrical angular frequency and electrical parameters of the 20-pole, 30-slot SRM are the same as those of the 8-pole, 12-slot SRM, as shown in Fig. 1 and Table I. With  $f_m$ ,  $N_m$ , and  $P$ , you can achieve the highest possible electrical frequencies while also achieving extremely fast rotational speeds. Model A has a maximum electrical frequency of 6.67 kHz, as seen in the graph (1). Model B calls for a total of 20 poles in order to achieve the same maximum electrical frequency as Model A at a maximum rotation speed of 20000rpm. These two SRMs have a comparable outer diameter, stack capacity, and air gap. These devices are also designed to have roughly equal self-inductance distribution, as seen in Figure 2. The torque of the SRM is measured in this way:

**Figure 2. Self-inductance waveform of the proposed SRMs.**

T, L, and I are the corresponding units for expressing the output torque, inductance,

electric angle, and phase current. A constant current is fed to all the poles, so that the resulting torque is proportionate to their number, as seen in (2). Model B has 2.5 times the torque of model A. For the same amount of torque, Model B requires 0.63 times as much current as Model A, as evidenced by (Fig. 3)

#### 4.

#### Controllability of Vector Control for SR

#### M

#### 4.1

#### Principle and current controller of vector control

Figure 4 shows the SRM vector control in action. A three-phase sinusoidal current with a DC offset is used as an excitation current. The AC section of the stator produces a rotating magnetic field. The DC part generates a rotating magnetic flux vector based on the rotor position. In the rotor field, the magnetic flux can be thought of as this flux vector.

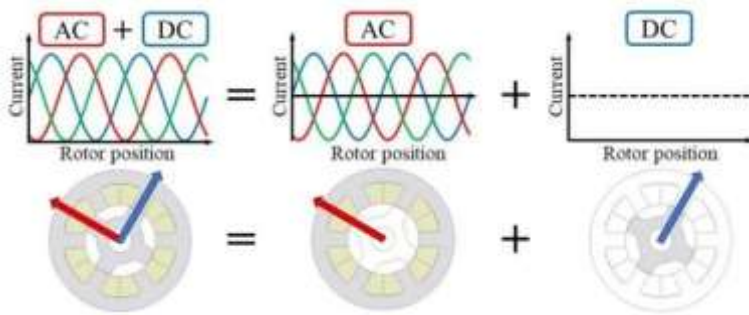
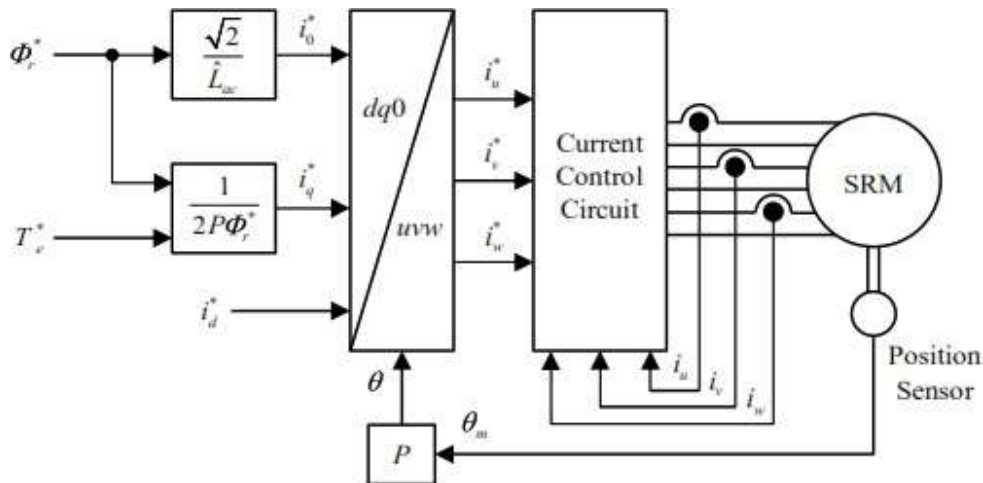


**Figure3.Vector control of SRM.**

When the spinning stator magnetic field and rotor magnetic flux interact, torque is generated for these purposes. The SRM's vector control torque production is described mathematically in the formulas [9-10]. The corresponding SRM voltage equation is

expressed using the d-q axis and zero-phase. Volts d are defined as the voltages  $v_d$ ,  $v_q$ , and zero-phase voltages; the currents of the d-axis,



q-axis and zero-phase currents; the winding resistance; the DC part of the self inductance; the self inductance amplitude. The d-axis volts are  $i_d$  and  $i_q$  and  $i_0$ ,  $R$ ,  $L_{dc}$  and  $L_{ac}$ , respectively. The DC component can be used to calculate the excitation current's zero-phase component, as shown in (3). The virtual rotor flux can be computed using the following equation using the second term inductance matrix of (3): where  $r$  is the virtual rotor flux. As can be seen in (4), the simulated

rotor flux is generated by zero-phase current. SRM's torque can be calculated as follows: According to (4) and (5), the rotor flux and torque currents are comparable to the zero-phase and q-axis currents (5).

**Figure4.Vector control system for SRM drive**

Extracted from (4) and (5), Figure 5 depicts the vector control system for the SRM drive (5).

How to use the new controller is discussed in [13]. Figure 6 depicts the brand-new vector control controller. Decoupling, feedforward controllers, and current PI controllers are all shown in Figure 6. The voltage directives from these controllers can be accommodated by a carrier-based PWM inverter. The PI controller regulates the current in each axis and phase component. According to the PI controller's transfer function of the transfer function of the PI controller's gain and the time constant

of time constant are written as  $G_{PI}$  and  $K_c$  in  $G_{PI}$ . RL circuits on the rotating reference frame can be characterized by decoupling and feed-forward controllers in the controlled-SRM. One-order current response is maximized by using a  $c$  equal to the regulated machine's time constant  $Ldc/R$ .  $K_c$  is a gain that is determined based on the current response speed. In this paper's simulation and trial, the new controller is used.

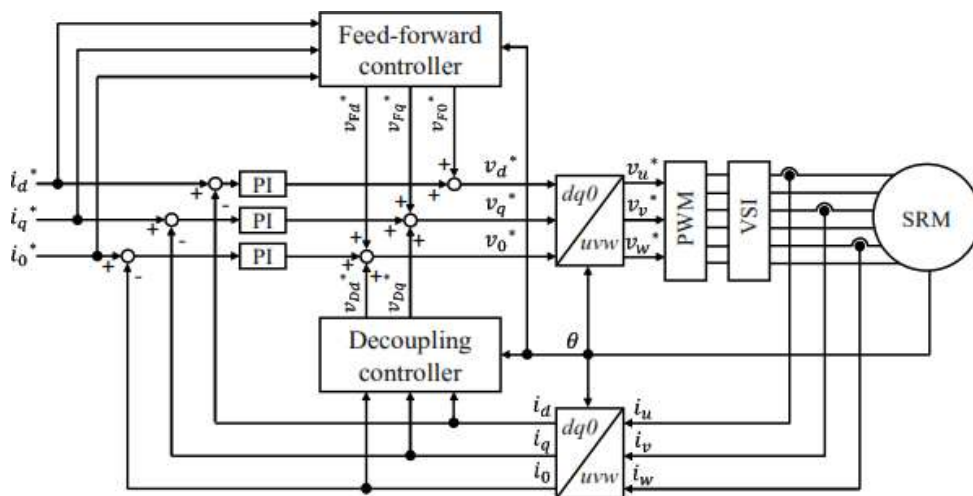
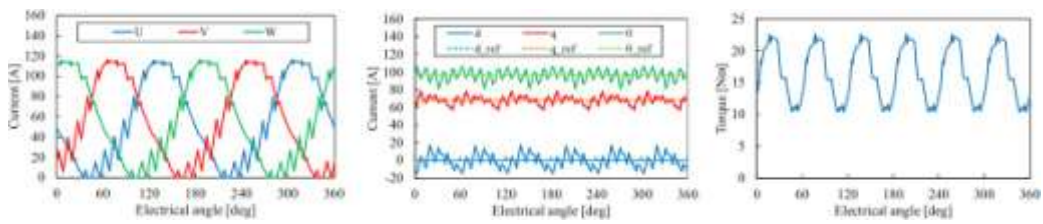


Figure 5. Current controller for vector control

#### 4.2 Controllability of high speed drive



4.3 For a 20000rpm rotational speed and a demand output power of 1 watt, the switching frequency and bus voltage are taken into account. Under the conditions of 20000 rpm and a reference torque of 16.2 Nm, the

actual waveform and torque waveform for the switching frequency are tested. Figure 7 depicts the switching frequency current and torque waveforms.

**Figure6.Current waveform and torque waveform depending on switching frequency (a) Three phase current (fsw=100kHz), (b) d-axis, q-axis, zero-phase current (fsw=100kHz), (c) Torque (fsw=100kHz)**

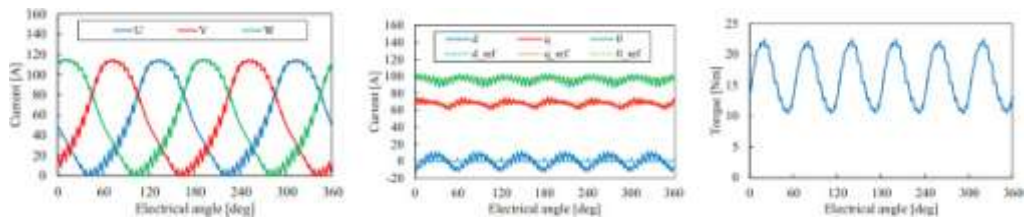


**Figure7.Current waveform and torque waveform depending on switching frequency (a) Three phase current (fsw=200kHz), (b) d-axis, q-axis, zero-phase current (fsw=200kHz), (c) Torque (fsw=200kHz)**

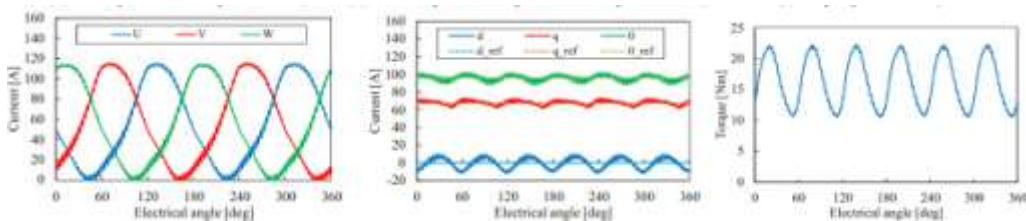


**Figure 8. Current waveform and torque waveform depending on switching frequency (a) Three phase current (fsw=333.3kHz), (b) d-axis, q-axis, zero-phase current (fsw=333.3kHz), (c) Torque (fsw=333.3kHz)**



Changing the switching frequency yields information on the overall harmonic distortion and the current ripple ratios. Total harmonic distortion (THD), current ripple ratio (CRR), and total harmonic distortion (THD) are abbreviations for each other. Each order harmonic current's effective value is shown in the table below. The current amplitudes  $i_{max}$ ,  $i_{min}$ , and  $i_{ave}$  represent the maximum, minimum, and average, respectively, of the current. Table II shows the q-axis and zero-phase THD and current ripple ratios for the switching frequency. Fig. 7 and Table II show a decrease in THD and current ripple ratio with increasing switching frequency. THD should be as minimal as feasible because harmonic fluxes in the high-speed drive increase iron loss. Switching frequencies between 100 kHz and 200 kHz provide a significant THD reduction ratio. On the other hand, at switching frequencies above 200 kHz, it hasn't made much progress. For optimal current ripple and THD, the number of switches each electrical angle cycle should be 30 or higher.

Consequently, the switching frequency has to be adjusted. Torque relationships can be realized in the simulation by accounting for the bus voltage required for their realization. In the simulation, the speed of rotation is set to 20000 rpm and the frequency of switching is set to 200 kHz. At a modulation ratio of less than 1, vector control is possible. When the modulation ratio exceeds 1.0, the vector control switches to single pulse driving. Vector control hence requires a voltage less than modulation ratio 1.0 for bus voltage. Increasing the vector control bus voltage raises the reference torque. The bus voltage must be 900V in order to achieve the 16.2Nm, 34kW. The high switching frequency required for vector control in the high-speed region is achieved using a SiC inverter, which was selected based on the simulation findings. This device has a rated power of 50kVA, an AC output current rating of 72.2Arms, a DC input voltage rating of 700V, and a maximum switching frequency of 200kHz

**Table 2. THD and Current Ripple Ratio**

1	Switching frequency [kHz]	100	200	333.3
2	3-phase current THD [%]	15.3	11.1	10.5
3	q-axis current ripple ratio [%]	32.2	21.0	17.2
4	zero-phase current ripple ratio [%]	26.3	16.6	14.7

## 5. Conclusion

Changing the switching frequency yields information on the overall harmonic distortion and the current ripple ratios. Total harmonic distortion (THD), current ripple ratio (CRR), and total harmonic distortion (THD) are abbreviations for each other. Each order harmonic current's effective value is shown in

the table below. The current amplitudes  $i_{max}$ ,  $i_{min}$ , and  $i_{ave}$  represent the maximum, minimum, and average, respectively, of the current. Table II shows the q-axis and zero-phase THD and current ripple ratios for the switching frequency. Fig. 7 and Table II show a decrease in THD and current ripple ratio with increasing switching frequency. THD should be as minimal as feasible because harmonic

fluxes in the high-speed drive increase iron loss. Switching frequencies between 100 kHz and 200 kHz provide a significant THD reduction ratio. On the other hand, at switching frequencies above 200 kHz, it hasn't made much progress. For optimal current ripple and THD, the number of switches each electrical angle cycle should be 30 or higher. Consequently, the switching frequency has to be adjusted. Torque relationships can be realized in the simulation by accounting for the bus voltage required for their realization. In the simulation, the speed of rotation is set to 20000 rpm and the frequency of switching is set to 200 kHz. At a modulation ratio of less than 1, vector control is possible. When the modulation ratio exceeds 1.0, the vector control switches to single pulse driving. Vector control hence requires a voltage less than modulation ratio 1.0 for bus voltage. Increasing the vector control bus voltage raises the reference torque. The bus voltage must be 900V in order to achieve the 16.2Nm, 34kW. The high switching frequency required for vector control in the high-speed region is achieved using a SiC inverter, which was selected based on the simulation findings. This device has a rated power of 50kVA, an AC output current rating of 72.2Arms, a DC input voltage rating of 700V, and a maximum switching frequency of 200kHz. Reference

[1]. IEEE Energy Conversion Congress and Exposition (ECCE) 2015, pp. 5241-5248: "Super-high-speed switching reluctance motor for vehicle traction," by M. Besharati, G. Atkinson, V. Pickert, and Jamie Washington.

"State-of-the-Art High-Speed Switched Reluctance Machines" by Earl W. Fairall, Berker Bilgin, and Ali Emadi, IEEE International Electric Machines and Drives Conference (IEMDC), pp.1621-1627, 2015.

[3]. A. Chiba, K. Kiyota, N. Hoshi, M. Takemoto, S. Ogasawara, "Development of a Rare-Earth-Free SR Motor with High Torque Density for Hybrid Vehicles," IEEE Transactions on Energy Conversion, vol.30, no.1, pp.175-182, March 2015.

In the Proceedings of the 19th International Conference on Electrical Machines and Systems 2016 (ICEMS 2016), K. Ueta and K. Akatsu, "Study of high-speed SRM with amorphous steel sheet for EV," Feb. 2017.

In-wheel electric vehicle use of a high-torque density permanent-magnet free motor, IEEE Transaction on Industry Application, vol. 48, no. 6, November 2012, pp. 2287-2295, S. P. Nikam, V. Rallabandi, and B G Fernandes [5].

Reluctance Switched Reluctance Machine Acoustic Noise Prediction: [6] IEEE Transactions on Industry Application, vol. 36, no. 6, pp.1589–1597, 2000. [6]

Chenjie Lin and Babak Fahimi, "Prediction of Radial Vibration in Switched Reluctance Machines,"

Volume 29, Number 1, Pages 250-258, 2014, IEEE Transaction on Energy Conversion

In "Digital PWMControl-Based Active Vibration Cancellation for Switched Reluctance Motors," by H. Makino, T. Kosaka and Nobuyuki Matsui, IEEE Transaction on Industry Application, vol. 51, no. 6, November 2015, pp. 4521-4530.

Proc. of 9th International Conference on Power Electronics and ECCE Asia (ICPE- ECCE Asia), June 2015.

IEEE Transactions on Industry Applications, 36, No. 1, pp. 111-121, January/February, 2000: [10].K. M. Rahman, B. Fahimi, G. Suresh,

**Author's Profile:**



S. Parveen Sulthana, Completed B. Tech In Electrical And Electronics Engineering In 2016 From A1 Global Institute Of Engineering And Technology Affiliated To JNTUK Kakinada And Pursuing M. Tech Form Dr. Samuel George Institute

A. V. Rajarathnam and M. Ehsani, "Advantages of Switched Reluctance Motor Applications to EV and HEV: Design and Control Issues,"

Of Engineering And Technologies Affiliated To JNTUK Kakinada, Andhra Pradesh, India. Area of interest Power Electronics (P.E). Email ID: spsulthana232@gmail.com



R. YEDUKONDALU He completed B.E in EEE at Sir C R R College of Engineering, Vatluru, and Eluru. He received his M. Tech in Control Systems from JNTUA, Anathapur and working as Associate Professor at Dr Samuel George institute of engineering and technology, Markapur, The Andhra Pradesh district of Prakasam. Control systems and renewable

energy sources are among his interests. Snail mail to: santoshpaul717@gmail.com